Int J. Heat Mass Transfer Vol. 21, pp. 1467–1479
0017-9310/78/1201-1467 $02.00/0

TRANSITION AND TRANSPORT IN A BUOYANCY DRIVEN FLOW IN WATER ADJACENT TO A VERTICAL UNIFORM FLUX SURFACE

Z. H. QURESHI and B. GEBHART
Department of Mechanical Engineering, State University of New York at Buffalo, NY 14260, U.S.A.

(*Received* 8 *August* 1977 *and in revised form* 6 *March* 1978)

Abstract—This experiment, in water at room temperature, accurately maps changes in the mean temperature distribution from laminar flow, through changes during transition, to full turbulent flow. Temperature disturbance levels are also determined. Simultaneously, very accurate measurements of local heat-transfer parameters were made to high Rayleigh numbers. Our objective was to interrelate different past criteria for the beginning of thermal transition and to find any characteristic patterns during transition. It was found that such criteria are internally consistent but some systematically disagree with others because of differences in methodology. Mean profiles and transport are relatively unambiguous. Further, some events during transition may also be correlated, from our measurements, both in terms of mean profiles and heat transfer. Transport in laminar, in transition and in turbulent flow are mapped. In the first regime, it agrees with theory and in the last, with the correlation of Vliet and Liu [1]. Mean temperature distributions in full turbulence are in very close agreement with the new transport theory of George and Capp [2].

NOMENCLATURE

B^*, characteristic frequency $= 50\pi f x^2/\nu G^{*2.5}$;
c, specific heat of water;
E, transition factor;
f, frequency [Hz];
g, acceleration due to gravity;
G, modified Grashof number $= 4(Gr/4)^{1/4}$;
G^*, modified flux Grashof number $= 5(Gr^*/5)^{1/5}$;
Gr_x, Grashof number $= g\beta(T_0 - T_\infty)x^3/\nu^2$;
Gr_x^*, flux Grashof number $= g\beta q_w'' x^4/k\nu^2$;
h, heat-transfer coefficient;
k, thermal conductivity of water;
Nu_x, Nusselt number $= hx/k$;
Pr, Prandtl number $= \mu c/k$;
q_w'', heat flux to plate;
Ra_x, Rayleigh number $Gr_x Pr$;
Ra_x^*, Rayleigh number $Gr_x^* Pr$;
T, temperature in boundary layer;
T_0, temperature of plate surface;
T_∞, ambient temperature;
T', temperature disturbance amplitude;
x, distance from leading edge of plate;
y, distance measured in boundary layer normal to plate;
z, distance measured in boundary layer parallel to plate.

Greek symbols

α, thermal diffusivity, $k/\rho c$;
β, coefficient of thermal expansion of water;
η, non-dimensional form of distance in boundary layer $= yG^*/5x$;
μ, dynamic viscosity of water;
ν, kinematic viscosity of water;
ϕ, non-dimensional form of temperature difference;
δ, boundary-layer thickness;
δ_h, enthalpy thickness $= \int_0^\infty \frac{T - T_\infty}{T_0 - T_\infty} dy$.

1. INTRODUCTION

BUOYANCY induced flows have been the subject of intense research in recent years. They are encountered in nature and in industry. Atmospheric and oceanic circulations are caused by buoyancy effects. The need for accurate prediction of transport abounds in industrial applications. In this study, a buoyancy induced flow along a constant flux vertical surface in water is investigated. Measurements are made in all the three flow regimes—laminar, transition, and turbulent. Thermal transport characteristics are measured over the whole range of conditions under which a laminar flow undergoes transition and becomes turbulent, due to hydrodynamic instability. We sought to clearly assess the meaning of conventional measures and to delineate their differences in terms of detailed transport mechanisms.

1.1. *Heat-transfer characteristics*

Heat transfer from a vertical heated surface is commonly correlated by the Nusselt number, Nu, as a function of the Grashof number, Gr. The Grashof number is a measure of the vigor of the induced flow, analogous to the Reynolds number of forced flow. The early study of Lorenz [3] analyzed laminar flow adjacent to an isothermal vertical surface, based on the assumption that the flow is laminar. Later analytical investigations used laminar boundary-layer theory. Similarity analyses gave compact, exact

and numerical solutions. Sparrow and Gregg [4] analyzed flow adjacent to a uniform heat flux vertical surface, which is the circumstance here. Calculations were compared to the experimental results of Dotson [5], with good agreement. The local Nusselt number, Nu_x, is a function of the modified Grashof number, $Gr_x^* = g\beta q_w'' x^4/kv^2$ where q_w'' is the uniform surface flux, and x is the distance from leading edge. This modified Grashof number is sometimes more convenient to compute, since the heat flux is known. In laminar flow, we may calculate the dependence of Nu_x on Gr_x^* for a given fluid Prandtl number.

The transport mechanisms in the transition region are very complicated. Heat-transfer characteristics vary during transition, and beyond, until a "developed" turbulence is established, see Bill and Gebhart [6]. Since turbulent flows are also of great practical significance, many experimental and analytical studies have also explored such thermal transport. The first calculated equation for turbulent flow adjacent to isothermal vertical surfaces was that of Eckert and Jackson [7], using an integral method. The resulting equation, below, is limited to Prandtl numbers close to 1.

$$Nu = 0.0246(Gr)^{2/5}(Pr)^{7.15} \times [1+0.494(Pr)^{2/3}]^{-2.5}$$

Earlier experimental work on eventual turbulent natural convection, by Griffiths and Davis [8], obtained local heat-transfer measurements for an isothermal surface in air. The heat transfer was found to be highest at the bottom section of the surface. It dropped to a minimum value further up and then rose to an almost constant value over the remaining section of the surface. Their explanation was, ". . .the laminar motion of the air persists up to a certain point only, beyond which turbulence sets in...". Saunders [9] investigated natural convection in water and mercury and surmised that the flow was not streamline for $GrPr > 10^{10}(Pr = 7.0)$. Above that limit, the heat-transfer correlation was found experimentally to be

$$Nu = 0.17(GrPr)^{1/3}.$$

Since this study, many workers have investigated turbulent flow along isothermal vertical surfaces. The results of Warner and Arpaci [10] in air are in good agreement with the analytical correlation of Bayley [11]:

$$Nu = 0.10Ra^{1/3} \qquad Ra \leqslant 10^{12}.$$

On the other hand, similar experiments by Cheesewright [12] in air appeared to support the Eckert and Jackson [7] result.

Surfaces dissipating uniform-flux have received less attention. Dotson [5] made measurements in air but they were limited to the laminar and transition regimes. Vliet and Liu [1] used a uniform-flux vertical plate in water. This data extended to a modified Rayleigh number (Gr_x^*Pr) of 10^{16}, over the range in Prandtl number from 3.6 to 10.5. Local heat transfer was correlated by

$$Nu_x = 0.568(Gr_x^*Pr)^{0.22}$$

The theoretical result of George and Capp [2] suggested that

$$Nu_x \propto (Gr_x^* \cdot Pr)^{1/4}.$$

We have obtained heat-transfer data for a uniform flux vertical surface in water. Our data spans the range from laminar flow, through the subsequent stages of transition, to full turbulence. The maximum modified Rayleigh number achieved was 5×10^{14}.

1.2. *Mean temperature profiles in turbulence*

The measurements of mean temperature across either a turbulent natural convection boundary region, or across a region in transition have been mainly in air on isothermal vertical surfaces. The measurements of Griffiths and Davis [8] were approximated by Eckert and Jackson [7] as follows

$$\frac{T-T_\infty}{T_0-T_\infty} = 1-\left(\frac{y}{\delta}\right)^{1/n}$$

where $n = 7$ and δ is the thermal boundary region thickness. Warner and Arpaci [10] concluded, from their measurements in air, that this is not an accurate representation. They suggested that, except at the wall itself, the profile is well represented on natural coordinates (physical distance from the wall) by a laminar profile over a great portion of the thermal layer. Cheesewright [12] also concluded that one-parameter similarity, in the sense in which it applies to the laminar boundary layer, cannot be used to scale the turbulent temperature profile across the boundary layer. Lock and de B. Trotter [13] made an experimental study of turbulent natural convection adjacent to a uniform-flux vertical plate immersed in water. Their temperature profiles were well represented by plotting the normalized temperature against physical distance from the plate, as suggested by Warner and Arpaci [10]. Vliet and Liu [1] divided the thermal boundary layer into three regions and suggested three separate relationships to represent the mean temperature distribution. They also concluded that the 1/7 power profile did not correlate their data either near the wall or in the outer portion of the thermal region.

Recently George and Capp [2] have analyzed fully developed turbulent natural convection boundary layers for both constant wall temperature and constant flux surface conditions. A detailed discussion is given on the absence of consensus concerning the scaling relations proposed in the past. They identified outer and inner flow regions and it was shown that the inner layer is a constant heat flux layer. This layer was seen, in turn, to consist of two major subdivisions. Near the wall is a conductive and viscous sublayer in which the mean temperature and velocity profiles are linear. A buoyant sublayer exists further out, where mean velocity and tempera-

ture profiles show respectively, a cube root and an inverse cube root dependence on distance from the wall. On dimensional grounds, scaling laws for the temperature and velocity fields were suggested.

We have made a large number of temperature measurements across the thermal layer, at different downstream locations and surface flux levels. As we will see the temperature profiles in the laminar region are in excellent agreement with the theory. In particular, the scaling laws appear to be well corroborated.

1.3. *Transition*

Most past investigations of natural convection flow along a heated vertical surface are concerned mainly with either the laminar or the fully developed turbulent regime. Laminar flow undergoes a complicated process of transition and adjustment before it becomes a "fully developed" turbulent flow. The heat-transfer characteristics and mean temperature distributions in the boundary layer gradually deviate from those of laminar flow and undergo a number of changes until the final trends are achieved.

The initiation of natural convection transition is similar to that in forced flow. However, the later stages of the process are different and far more complicated and varied. A natural convection flow first becomes unstable to small disturbances as soon as it has reached a certain value of Gr_x, as indicated by linear stability theory and confirmed in detail by measurements. Ever-present disturbances amplify downstream under the conditions where a balance of buoyancy, pressure and viscous forces contribute energy to such disturbances. Such highly amplified disturbances are the cause of later breakdown. The analytical and experimental investigations concerning laminar instability were summarized by Gebhart [14].

Vliet and Liu [1] studied flow adjacent to a uniform heat flux vertical surface in water. They defined the beginning of transition to be the downstream location where the measured surface temperature begins to decrease, that is, after the maximum surface temperature is reached. Cheesewright [12] made some measurements in the transition regime in air. The criterion for the beginning of transition was taken to be the appearance of significant temperature fluctuations in the boundary layer.

Past studies indicate wide ranges of Grashof number over which the beginning and the end of transition occur. The Grashof number Gr_x^* is, for some purposes, more conveniently related to G^* as $G^* = 5(Gr_x^*/5)^{1/5}$. Lock and de B. Trotter [13] suggested $G^* = 320$–525 ($Pr = 9.9$–11.85) for the beginning of transition and $G^* = 550$–750 for its end, in water. Estimates of G^* by Vliet and Liu [1] in water were 800–1300 and 1150–2000, respectively, for data at $Pr = 10.5$–3.6. Linear stability theory and measurements show that the growth rate of two-dimensional disturbances depends upon the local Grashof number, G^*.

The large spread in G^* posed the question of whether or not a systematic trend possibly exists, dependent perhaps on the heat flux q_w''. Godaux and Gebhart [15] measured the beginning of the thermal transition process at different heat flux levels in water and found conclusively that it is not correlated by the use of Grashof number alone. For the different heat flux levels used, thermal transition was always found to occur at the downstream location x where the product $Q = q_w''x$, i.e. the total amount of thermal energy given to the boundary layer by the heated surface, had reached approximately the same value. In terms of G^*, this is a constant value of $G^*/x^{3/5} \propto (q_w''x)^{1/5}$. For the end of transition, a range of G^* was suggested.

More recently, Jaluria and Gebhart [16] made detailed measurements of the beginning and progress of transition in water. Both the velocity and temperature fields were determined. Criteria for the beginning of both velocity and thermal transition were established. They characterized the thermal transition events by G^*/x^n, where n appeared to be 0.4 and 0.54 for the beginning and the end of transition, respectively. The first limit is proportional to the local kinetic energy flux $E = G^*(\nu^2/gx^3)^{2/15}$. They found that $E = 13.6$ and 15.2 for the beginning of velocity and thermal transition, respectively. To assess the general validity of the parameter E, as a correlator of the beginning of transition, they collected all transition data from previous studies in air and in water. A 70% spread in E, over a Prandtl number range from 0.7 to 11.85, was found. This spread is clearly due, in part, to the past use of differing criteria and judgement in the matter of assigning the actual location of the beginning of transition, and in the ways the locations were determined experimentally.

The present study considers, in detail, the effects of different methods of specifying or determining the beginning of thermal transition. Successive transition events are interpreted according to several measures; linear stability theory predicted amplification downstream, deviation of the mean temperature distribution in the boundary layer and heat-transfer characteristics. Our results are well correlated by the transition parameter E, suggested by Jaluria and Gebhart [16] but the numerical value of E varies according to the criterion used in defining the beginning of thermal transition.

2. APPARATUS

A buoyancy induced flow was generated in water along a vertical surface dissipating a constant heat flux. The surface assembly consists of two 0.00127 cm thick, 130.5 cm long and 46.6 cm wide Inconel 600 foils separated by layers of Teflon. Twenty four, 127 μm copper–constantan thermocouples were placed along the vertical centerline (in the middle of the Teflon layers) of the plate. The whole plate assembly had

been heated under high pressure to fuse the Teflon to the foil. The resulting thickness was 0.038 cm. The plate was then stretched vertically between two stainless steel knife edges. The whole assembly was supported by a stainless steel frame sitting in a $1.83 \times 0.662 \times 1.83$ m high insulated tank made of stainless steel, with glass windows. The leading edge of the plate was 20 cm from the bottom of the tank. The tank was filled with water of high purity, approximately 1.5 mΩcm resistivity, to eliminate the possibility of electrolysis, electrical leakage and any drift in the probe used. For the present study, pure water was obtained by an apparatus capable of converting tap water into pure water of resistivity about 4 mΩcm at a rate of 1 gal/min Water was deaerated by passing it through at 63 cm Hg vacuum chamber. To avoid the contamination of water only

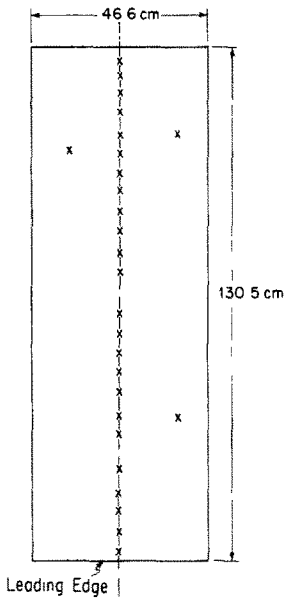

FIG. 1 Thermocouple locations in the plate assembly

stainless steel, Teflon, silicon glue and silicon grease were allowed to come in contact with it.

The resistance of the plate was measured by connecting it in series with a known precise resistor and passing a trickle current through it. The voltage measurements gave the plate resistance. It was also checked by an accurate wheatstone bridge. The two measurements agreed to within 0.1%. The plate assembly was heated by a Hewlett–Packard 6475C D.C. power supply capable of supplying 0–110 V and 0–100 A. To study the detailed development of turbulent transport, Bill [6] heated the same plate to a maximum flux of 1920 W/m^2 and $G^* = 1574$. Most of this data corresponds to the transition, although some is in the turbulent region. We were able to attain a heat flux of 4488 W/m^2 and a maximum value of $G^* = 2164$. The surface flux was calculated from the measurement of voltage drop across the foil and the current flowing through an accurate resistor in series with the plate. The uniform thickness of the foil assured the uniform surface flux condition.

The thermal capacity of the foil was sufficiently small so the transient start-up time was limited to 1–2 min, depending upon the surface heat flux. The large volume of the tank enabled us to run the experiment for 30 min without causing appreciable ($\sim \frac{1}{4}$°C) thermal stratification and circulations in the tank.

Only the temperature measurements along the vertical surface and traverses across the boundary layer were required in the present study. The traverses were made by 0.0127 mm dia chromel–alumel thermocouple using a reference temperature of 0°C. The thermocouple probe was attached to a manual sliding mechanism capable of traversing the thermocouple in all the three directions. The surface temperature at different locations downstream from the leading edge were measured by the corresponding thermocouples embedded in the plate assembly. See Fig. (1) for thermocouple locations in the plate assembly. The thermocouple signals were recorded on a Beckman four-channel R511 Dynograph. All 24 surface thermocouples were connected to an Omega miniature thermocouple jack panel. A 28 point, two-pole, Omega Rotary Thermocouple Selector Switch selected the output signal recording. The two-pole switches are preferred as they do not allow a bad thermocouple to affect the output of the other thermocouples. The response time of the surface thermocouples was of the order of 10 ms. This was adequate for the frequencies encountered in this study. The output of the boundary-layer thermocouple was recorded on two channels– one for the time average temperature at different locations across the boundary layer and the other one for the instantaneous temperature disturbances. Eight thermocouples were suspended vertically in the tank at different x-locations (about 30 cm from plate) to indicate any thermal stratification, characteristic of circulations in the ambient medium.

The heat-transfer and boundary-layer measurements were taken by traversing the thermocouple probe across the boundary layer at different downstream locations x, each at different surface heat flux levels. Six downstream locations were selected to study the events and, for each location, measurements were made for ten different levels of heat flux q''_w. This resulted in data over a wide range, $G^* = 41$–2164. The accurate positioning of probe from the surface was extremely important due both to the thin thermal boundary region and the sharp temperature gradients in it. The location of the surface was determined by the completion of a resistance circuit containing the surface itself and two stainless steel capillary tubes, adjacent to and parallel to the probe. The least count on the traversing mechanism in any direction was 0.0025 cm.

All the experiments were performed late at night to avoid any large disturbances caused by daytime

activity in the building. At the end of every experiment, the water in the tank was stirred thoroughly to eliminate any temperature gradients. Then 2–3 h were allowed for any disturbances and circulations to dampen out before the next experiment was performed. The data were computer reduced immediately after the experiment. The laminar data were verified with the theoretical results. After establishing the consistency and reproducibility of the results, the rest of the measurements were carried out.

of laminar flow. Increasing turbulence increases the local heat-transfer coefficient h_x and causes a drop in the local surface temperature, which gradually falls to a minimum value. Thereafter, it slowly increases with the downstream distance, indicating a corresponding decreasing heat-transfer coefficient. Three flow regimes may be identified from the trends of $(T_0 - T_\infty)$ seen in Fig. 2. The highest value of $(T_0 - T_\infty)$ attained during the experiments was 14.2°C. Recall that h_x is proportional to the inverse of $(T_0 - T_\infty)$. Vliet and Liu [1] considered the beginning of

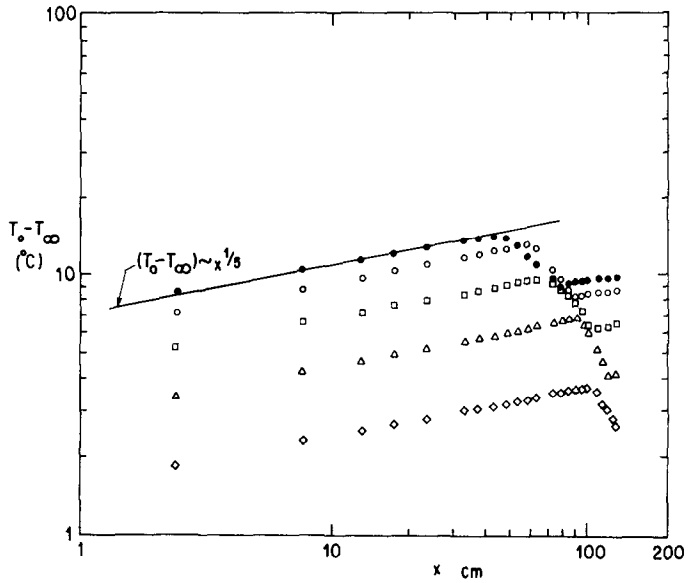

FIG. 2. Surface temperature variation with downstream distance from the leading edge. ◇, $q''_w = 583\ \mathrm{W/m^2}$; △, $q''_w = 1323\ \mathrm{W/m^2}$; □, $2326\ \mathrm{W/m^2}$; ○, $3714\ \mathrm{W/m^2}$; ●, $4488\ \mathrm{W/m^2}$.

3. EXPERIMENTAL RESULTS

3.1. *Local heat-transfer measurements*

Local heat-transfer measurements were made over the surface heat flux range $150 < q''_w < 4488\ \mathrm{W/m^2}$. The local surface temperature was recorded by 24 copper–constantan thermocouples embedded in the surface along the vertical center line. The first was at $x = 2.4$ cm and the last one was at $x = 127.4$ cm, see Fig. 1. Our data range is $G^* = 41$–2164 or $Ra_x^* = 1.2 \times 10^6$–5.1×10^{14}. The ambient temperature was always in the range from 22 to 24°C. The fluid properties were evaluated at the film temperature, the average of the ambient and local wall temperatures, T_∞ and T_0. The temperature, T_0, was averaged over 30 s in the laminar region and 60–150 s for the transition and turbulent regimes. Some of the tests were repeated for a longer recording time and the averages of the local surface temperatures were verified.

The local surface temperature excess $(T_0 - T_\infty)$ as a function of downstream distance from the leading edge, for several heat flux levels, is shown in Fig. 2. It increases as $x^{1/5}$ in the laminar region, as predicted by theory. Further downstream, the flow begins gradual transition to turbulence. The transport characteristics progressively deviate from those transition as the location where the surface temperature reaches its maximum value. We have found that the departure of surface temperature from the laminar trend begins well before it reaches the maximum value. The question of assigning the location of maximum surface temperature as the beginning of transition will be discussed later.

One of the most important aspects of transition is this effect on heat transfer. For the laminar regime, boundary-layer theory predicts, for a Prandtl number of 6,

$$Nu_x = 0.839(Gr_x^*)^{1/5} = 0.587(Ra_x^*)^{1/5}.$$

Figure 3 compares this with the measured local heat transfer. Excellent agreement is evident.

A sample of our measurements of local heat transfer before, through, and after transition are shown in Fig. 4. The deviation from laminar occurs in the region from $Ra_x^* = 1.2 \times 10^{13}$–$4 \times 10^{13}$, depending on the heat flux level. The end of each transition, into a single higher trend, occurs in the region between $Ra_x^* = 5 \times 10^{13}$ and 10^{14}. Vliet and Liu [1] observed the same transition characteristics. However, deviation began in the range between $Ra_x^* = 3 \times 10^{12}$ and 4×10^{13} and ended between 2×10^{13} and 10^{14}. These upper limits agree more closely with

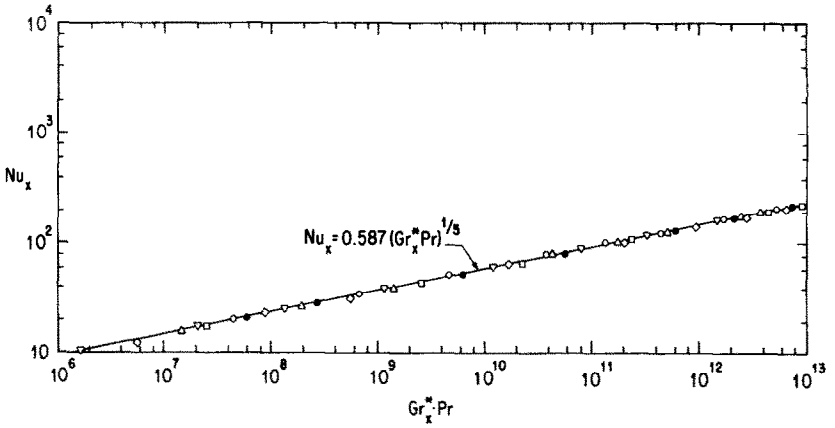

FIG. 3. Local heat-transfer data in laminar regime. ▽, $q_w'' = 148\ W/m^2$; ◇, $q_w'' = 583\ W/m^2$; △, $q_w'' = 1323\ W/m^2$; □, $q_w'' = 2326\ W/m^2$; ○, $q_w'' = 3714\ W/m^2$; ●, $q_w'' = 4488\ W/m^2$.

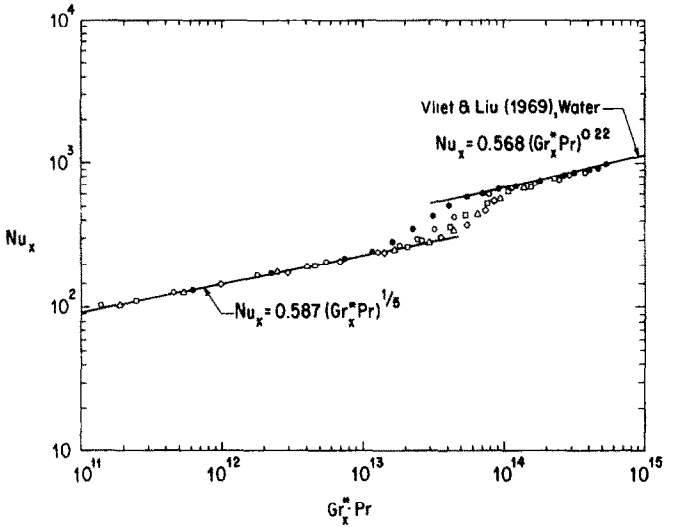

FIG. 4. Local heat-transfer data in transition and turbulence. Symbols are same as in Fig. 2.

ours than do the lower ones. The occurence of early transition and turbulence observed by Vliet and Liu [1] may be due to a different experimental situation and Prandtl number for most of the data.

Figure 4 clearly shows the dependence of the range of the transition process on the level of surface heat flux. Increasing flux results in an earlier beginning and completion. This is predicted by the transition criterion E. That is, transition occurs for $q_w'' x^2$ nearly constant. Transition will be discussed in detail in later sections.

Of most practical significance is the transport relation in the turbulent regime. Many correlations have arisen. Most pertain to the isothermal surface condition for which the local Nusselt number and Grashof number are related approximately by $Nu_x \sim (Gr_x Pr)^m$. Different values of m have been suggested. Eckert and Jackson [7] arrived at $m = 0.4$. Bayley [11] calculated $m = 1/3$. It is reasonable to expect that a turbulent heat-transfer correlation for an isothermal surface would apply approximately to a uniform-flux surface, since the surface temperature remains almost constant after passing through a local minimum in the transition regime.

For a uniform flux surface, local Nusselt number is taken as dependent on the flux Grashof number Gr_x^*. This is merely the product of the ordinary Grashof number and Nusselt number. Vliet and Liu [1], using a constant flux plate in water, also observed an increasing downstream surface temperature in full turbulence, as did we. They correlated local heat transfer by

$$Nu_x = 0.568 (Gr_x^* Pr)^{0.22} \quad 2 \times 10^{13} < Ra_x^* < 10^{16}.$$

Our data is also correlated very well with this correlation, as seen in Fig. 4. Our data also shows that fully developed turbulent flow is always present by $Gr_x^* Pr = 10^{14}$, even at very low flux level.

3.2. *Mean temperature distributions*

Mean temperature profiles were obtained at six downstream locations, $x = 43.3$, 58.0, 63.3, 78.6, 98.9, and 119.4 cm. At each, experiments were carried out at surface heat flux q_w'' levels of 150, 333, 590, 920, 1325, 1785, 2325, 2940, 3540 and 4488 W/m^2, that is, 60 experiments. Past studies of the temperature field used different methods to measure the surface temperature T_0. Godaux and Gebhart [15] pushed a thermocouple against the surface. Jaluria and Gebhart [16] determined it by extrapolation, to the

surface, of the measurements of mean temperature in the flow. We measured it by the thermocouples embedded in the surface assembly as done in [1]. No temperature gradient existed across this assembly as both sides of the surface dissipated an equal amount of heat and streamwise conduction was negligible. High accuracy is required, since the distribution of local temperature excess is normalized by the surface temperature excess $T_0 - T_\infty$ to yield ϕ.

Figure 5 shows mean temperature distributions in what we found to be the laminar regime, in terms of the appropriate similarity variable η. The laminar boundary-layer solution is also plotted, for $Pr = 5.7$. Excellent agreement is seen.

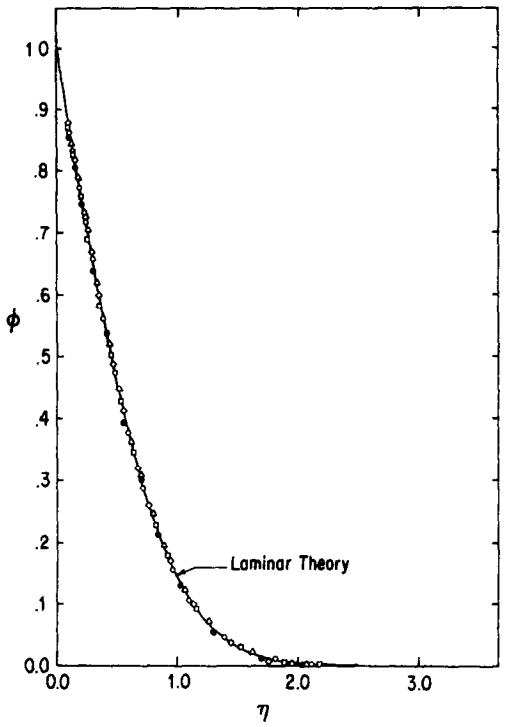

FIG. 5. Temperature profile in laminar boundary layer. The five experiments shown are denoted by ●, △, ○, ◇ and □, for which $q''_w = 148, 333, 586, 613$ and $919\ \mathrm{W/m^2}$, $x = 0.633, 0.580, 0.433, 0.580$ and 0.433 m resulting in $E = 12.66, 14.62, 14.43, 16.60$ and 16.01 respectively.

With the beginning of transition, the mean temperature distribution begins to deviate from the laminar one. With increasing G^* the profiles steepen near the surface and flatten at higher η. The thermal boundary-layer thickness increases from the laminar trend. This variation and development is shown in Fig. 6. For each profile, the corresponding kinetic energy flux parameter $E \sim G^*/x^{2/5}$ of Jaluria and Gebhart [16], was calculated. The numerical value, E, increases as transition proceeds. Our data suggests that the mean temperature distribution first deviates appreciably from the laminar one when $E = 19.2$. It adjusts to an unchanging fully turbulent one when $E = 28.0$–29.0. For each profile, the corresponding values of q''_w and x are also shown in Fig. 6.

These results suggest an added role for the parameter E, during transition. Note for example, that the middle two distributions are quite similar. The second was at 78% higher heat flux, but the value of E is only 14% greater.

Mean temperature distributions in the fully turbulent regime are shown in Fig. 7. Normalized temperature is plotted against the physical distance from the wall. The corresponding values of Ra^* and E are also shown for each profile. The effect of increasing E is only the thickening of the thermal boundary layer. An interesting feature of these profiles is their similarity close to the wall. However, further out, they diverge, due to increasing thickness of the thermal layer. Similar characteristics were observed by Warner and Arpaci [10], Cheesewright [12] and Jaluria and Gebhart [16].

Many attempts have been made in the past to correlate mean temperature distribution ϕ, in turbulent boundary layers, as a function of dimensionless distance from the wall. Cheesewright [12] tried $(y/x)Gr^{0.1}$ without success. Vliet and Liu [1] used

$$\delta_h = \int_0^\infty \frac{T - T_\infty}{T_0 - T_\infty} \mathrm{d}y \text{ in } y/\delta_h$$

and proposed three correlations to characterize the thermal boundary layer. George and Capp [2] have shown that δ_h is neither an inner nor outer scale but a mixture of both. (Cf. equations 88–91 of George and Capp [2].) Jaluria and Gebhart [16] showed conclusively that even the measured thermal boundary thickness could not successfully scale the distance from the wall.

George and Capp [2] attributed these failures to a need to determine which dimensionless groups govern and which physical phenomena dominate. They concluded that the temperature and velocity scales for the inner and outer regions are different.

They suggested inner and outer layers in the flow. Very near the wall is a conductive viscous sublayer in which the mean temperature and velocity profiles are linear. The outer part of the constant flux layer is the buoyant sublayer. There, the mean temperature and velocity profiles show, respectively, a cube root and an inverse cube root dependence on distance from the wall. Both temperature trends are plotted in Fig. 7. Our temperature data strongly confirm the characterizations of temperature decay in the constant flux layer.

This matter is considered in more detail as follows. On dimensional grounds, scaling laws for conductive and buoyant regions were suggested. In the conductive sublayer, the mean temperature distribution is given by

$$\phi = 1 - \frac{q''_w}{k(T_0 - T_\infty)} y.$$

The characteristic length scale then being $k(T_0 - T_\infty)/q''_w$. Figure 8 shows this prediction and our temperature data near the wall. The agreement, both in level and trend, is very good.

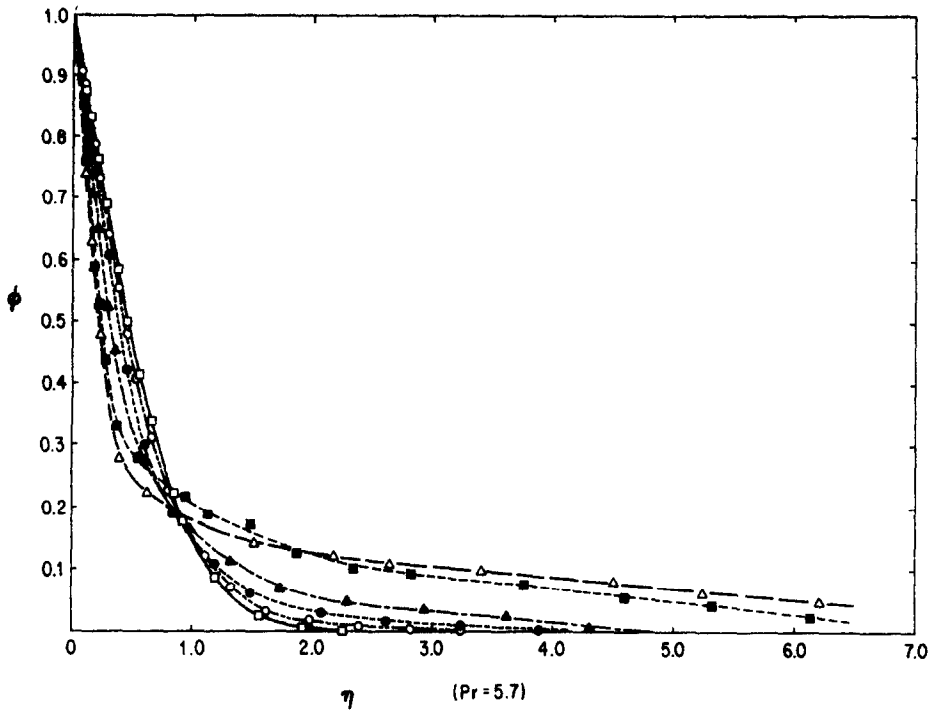

FIG. 6. Mean temperature distribution in transition from laminar to turbulent flow. The six experiments shown are denoted by □, ○, ●, ▲, ■ and △, for which q''_w = 1324, 2324, 1327, 2368, 2973 and 3639 W/m^2, x = 0.433, 0.433, 0.786, 0.786, 0.786 and 1.194 m resulting in E = 17.15, 19.4, 22.47, 25.59, 27.06 and 32.11 respectively.

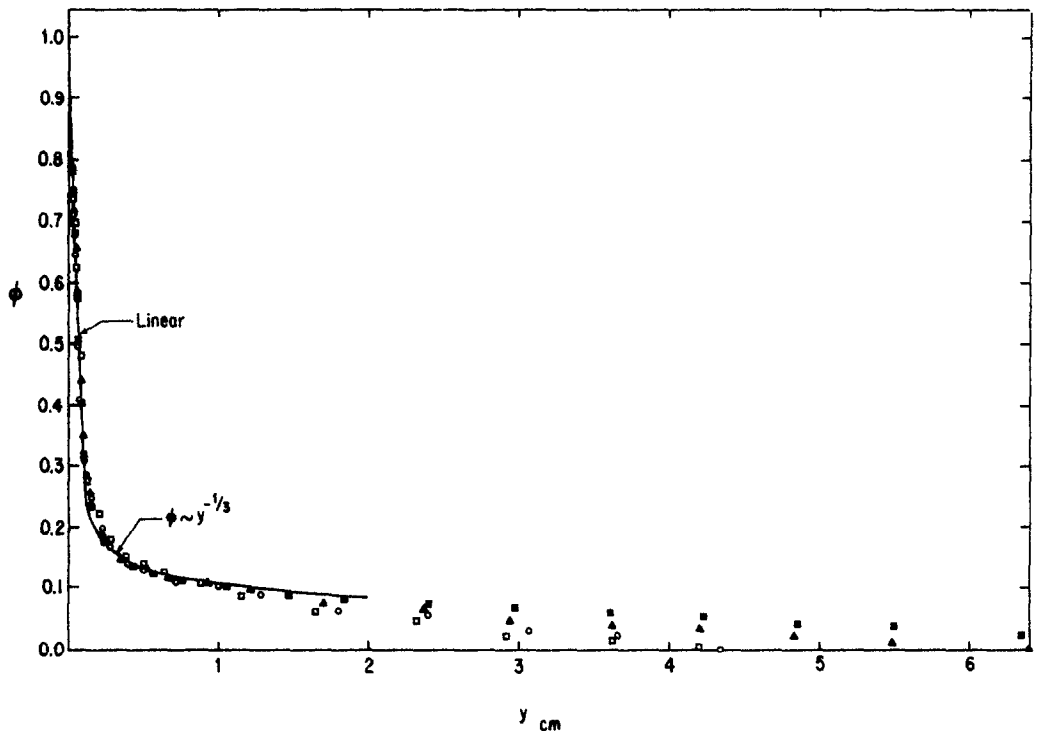

FIG. 7. Mean temperature distribution in turbulent boundary layer.

Symbols	q''_w (W/m^2)	x (m)	Ra^*_x	E
□	2326	1.194	1.62×10^{14}	29.32
○	3663	0.989	1.36×10^{14}	30.45
▲	3639	1.194	2.55×10^{14}	32.11
■	4488	1.194	3.28×10^{14}	33.74

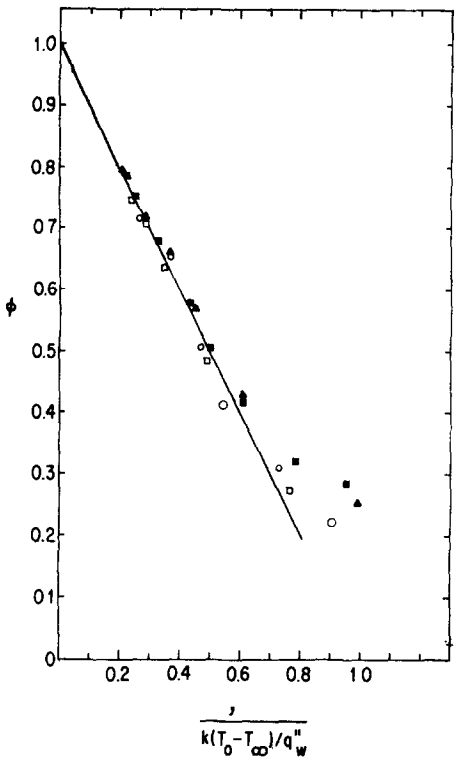

FIG. 8. Mean temperature profile in region near wall. Symbols are same as in Fig. 7.

For the buoyant sublayer, the length scale is $[k\alpha^2/g\beta q_w'']^{1/4}$ and the temperature scale is $[q_w''^3\alpha^2/g\beta k^3]^{1/4}$. The mean temperature distribution in this region is then written as

$$\frac{T_0 - T_\infty}{\left[\frac{q_w''^3\alpha^2}{g\beta k^3}\right]^{1/4}} = C\left(\frac{y}{\left(\frac{k\alpha^2}{g\beta q_w''}\right)^{1/4}}\right)^{-1/3} + D(Pr).$$

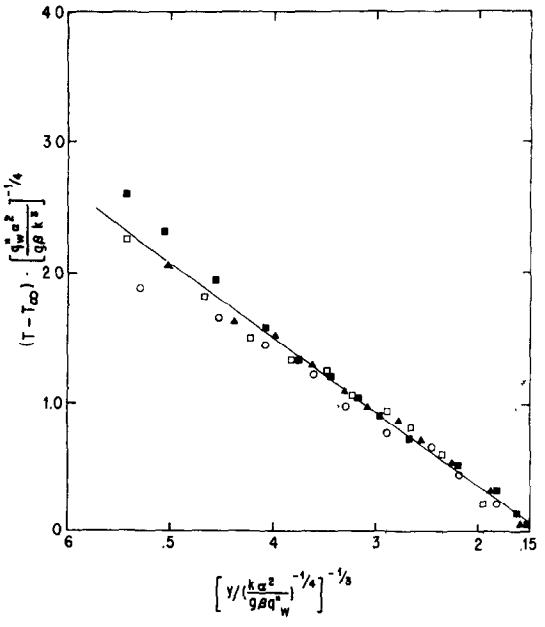

FIG. 9. Mean temperature distribution in buoyant sublayer. Symbols are same as in Fig. 7.

Figure 9 shows this prediction and our temperature data in the buoyant region. The agreement is again very good. Our least square determination gives $C = 5.65$ and $D = -0.76$ for $Pr = 6$. The value of C is in good agreement with $C = 5.6$ obtained by George and Capp [2] from the data of Cheesewright, Smith and Fujii.

The temperature data of Vliet and Liu [1] in the turbulent regime was reduced using the temperature and length scales proposed by George and Capp [2]. Their data very near to the wall does not agree with theory. However, in the buoyant sublayer it is in good agreement.

3.3. *Transition mechanisms*

When mean temperature distributions were determined from an averaged analog signal, temperature disturbances were recorded simultaneously on a separate channel using a higher gain, depending upon the magnitude of the disturbance. These records showed the amplification of the ever-present disturbances, as they are convected downstream. As a general disturbance is convected along, it is filtered for a predominant component, called the characteristic frequency (see Gebhart and Mahajan [17]). The non-dimensional frequency is defined by Gebhart and Mahajan [17] as

$$B^* = \beta^* G^{*1/2} = 2\pi f(g\beta q_w''/k\nu^2)^{-1/2}$$

for a uniform surface flux condition. The value of B^* at the characteristic frequency is essentially a single value for a given fluid Prandtl number. The concentration of disturbance energy at this frequency eventually causes transition. Nonlinear and three-dimensional effects arise, transition begins, and the laminar flow is consumed rapidly into complete turbulence. See the calculations of Audunson and Gebhart [18].

The characteristic frequency values for a uniform flux surface in water ($Pr = 6.7$), based on stability theory, is about 0.675. Our temperature disturbance data strongly confirms the frequency filtering mechanism. Figure 10 shows the most highly amplified frequency path on the stability plane (Hieber and Gebhart [19]). The analog records of our experiments have yielded the data points shown. The first appearance of natural oscillations were approximately at $A = 7$ where A is the amplitude ratio.

Figure 11 is an analog record of the amplification of natural oscillations as the laminar flow undergoes transition at one constant value of surface flux level. As the disturbance is convected downstream, its frequency and amplitude increases. The natural oscillations are almost sinusoidal but downstream they are distorted. We know that secondary mean motions arise, Jaluria and Gebhart [16]. Turbulent bursts then appear which eventually completely consume the laminar flow. At this stage, no single frequency contains a preponderance of the disturbance energy.

At any particular downstream location x, the disturbance level varies across the boundary layer.

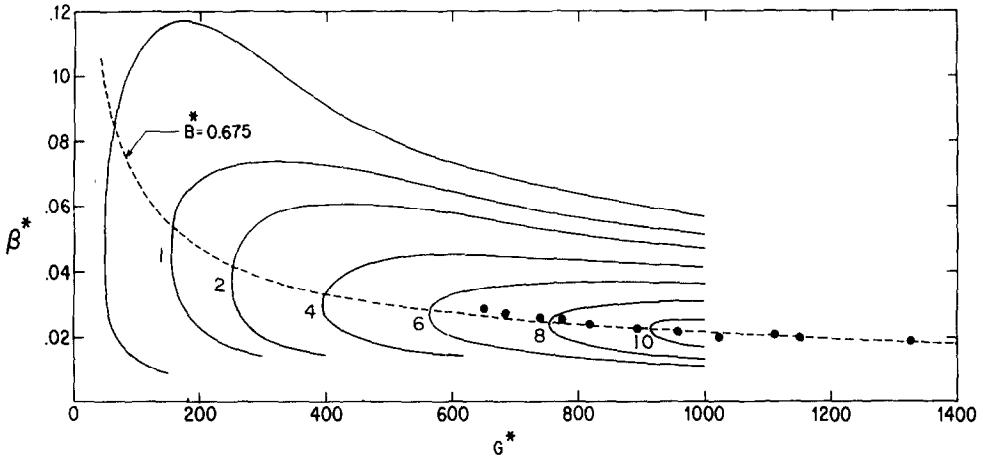

FIG. 10. Stability plane for $Pr = 6.7$ (Hieber and Gebhart [19]) showing amplitude ratio contours in the unstable region, -----, characteristic frequency path for $B^* = 0.675$. ●, data points of present study.

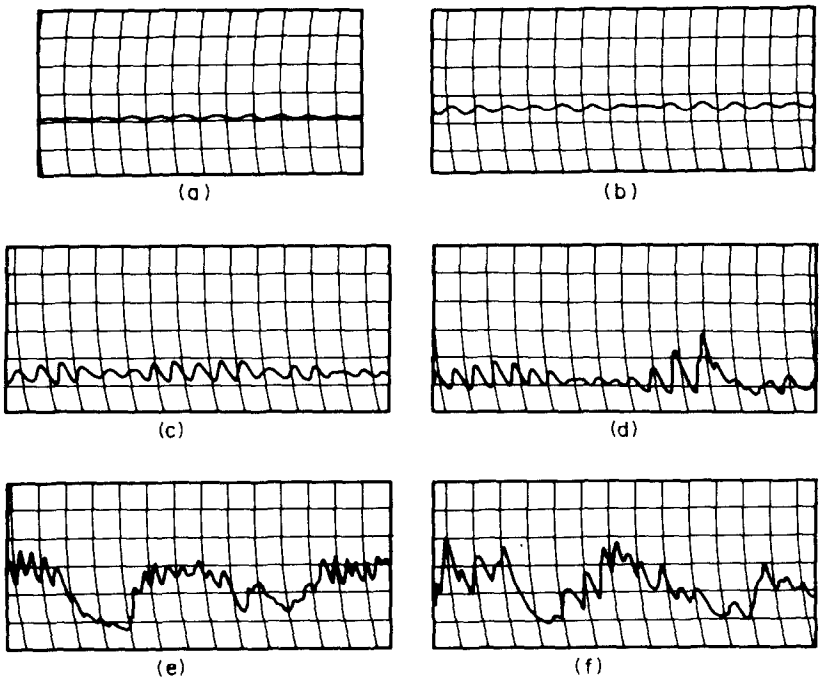

FIG. 11. Analog record of amplification of natural oscillations as the laminar flow undergoes thermal transition $q''_w = 1325\,W/m^2$. (a) $E = 17.5$, (b) $E = 19.6$, (c) $E = 20.45$, (d) $E = 22.47$, (e) $E = 24.46$, (f) $E = 26.01$

Its amplitude T' is known to be maximum near the maximum of the laminar velocity profile. Our temperature disturbance amplitude data across the boundary layer, in the transition region, are plotted at different downstream locations, in Fig. 12. The disturbance profile calculated by Dring and Gebhart [20] is also shown. The local disturbance amplitude T' is divided by its maximum amplitude across the boundary region. As the disturbances are convected downstream, the maximum of the profile shifts towards the surface and the temperature disturbances penetrate further out. These trends were also reported by Jaluria and Gebhart [16] and by Godaux and Gebhart [15].

4. CONCLUSIONS

During thermal transition, the heat transfer characteristics and mean temperature distributions gradually adjust from the laminar trends to the turbulent ones. For the practical estimate of heat transfer and other flow characteristics, we must differentiate and correctly predict the several flow regimes. We have reviewed the different methods of specifying or determining the beginning of thermal transition. Criteria such as the appearance of significant temperature fluctuations and the location where the measured surface temperature reached its maximum value are among the precise ones to date. However, thermal transition follows the amplifi-

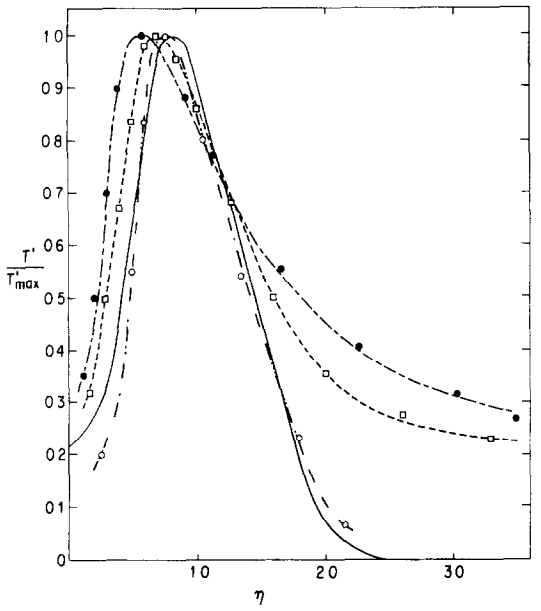

FIG. 12. Variation of the amplitude of the temperature disturbance T' across the thermal boundary layer at q''_w = 2370 W/m^2. ——, disturbance profile calculated by Dring and Gebhart [20]. The three experiments are ○, □, and ● for which x = 0.580, 0.633 and 0.786 m and E = 22.46, 23.40 and 25.59 respectively.

cation of ever-present disturbances and occurs even after the first appearance of fluid mechanic turbulence.

Our data is the wide range of G^* = 41–2164, from laminar flow to full turbulence. They confirm the validity of the parameter E as the correlator of the beginning of transition in water. They also indicate that subsequent events in transition are also, at least approximately, correlated by E. At E = 17.5, the temperature disturbances were found to have reached a level of 5% of $T_0 - T_\infty$. These disturbances increase the thickness of the thermal boundary region. However, the slope of mean temperature profile at the surface does not change significantly. The deviation of the mean temperature profile first became appreciable at all flux levels around E = 19.2. Measurable fluctuations in the surface temperature T_0 were also recorded. There had been a slight deviation of T_0 from the laminar trend, before reaching its maximum value. The maximum surface temperature occurred at E = 22.7 within an RMS of 0.61 in all the experiments. The value of E corresponding to maximum surface temperature measurements made by Vliet and Liu [1] is calculated to be 16.3–24.0 over the wide range of Prandtl numbers from 3.6 to 10.5. After this stage, the mean temperature field drastically deviates from the laminar trends. The slope gradually increases at the wall. Turbulent mixing increases the thermal region thickness.

Figure 13 shows the limits of each of these different transition events on a $G^* \sim q''_w$ plot. The constant E-parameter loci correlate each event. These lines on these coordinates have a slope of 1/5. They determine the local flow regime for any given value of surface flux level and local Grashof number.

Our determinations have resulted in relatively sharp limits for different modes of transport. We define the beginning of the transition of thermal transport as the condition under which the mean temperature distribution across the boundary layer begins to deviate from that characteristic of laminar flow. Our data suggest E = 19.2 for this limit. Achievement of the completely turbulent trend in heat transfer inferred from the $Nu_x \sim Gr_x^*$ plot, fell in the range of E = 28–29. However, the data was not sufficient in quantity to sharply determine detailed variation of the limit.

Finally, our mean temperature distributions have corroborated very well some surmises of George and

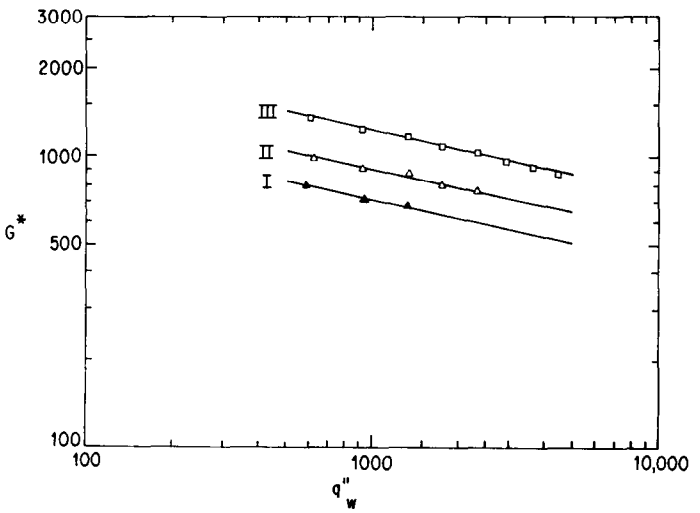

FIG. 13. Events of thermal transition. I—E = 17.5 Temperature disturbance found in boundary layer, T' = 0.05 ($T_0 - T_\infty$). II—E = 19.2 Deviation of mean temperature profile from laminar trend. III—E = 22.7 Maximum surface temperature.

Capp [2] concerning turbulent transport mechanisms in such a flow. The data follows predicted trends very closely and we have been able to evaluate an undetermined constant in their formulation.

Acknowledgements—The authors wish to acknowledge support for this study by the National Science Foundation under Grant ENG 7522623. We would also like to acknowledge the expert continuing efforts of Donna George in the preparation of the manuscript.

REFERENCES

1. G. C. Vliet and C. K. Liu, An experimental study of turbulent natural convection boundary layers, *J. Heat Transfer* **91**, 517–531 (1969).
2. W. K. George, Jr. and S. Capp, The natural turbulent boundary layer on a vertical flar plate, to be presented at Winter ASME Meeting Session 16 (1977).
3. L. Lorenz, *Ann. Phys.* **13**, 582 (1881).
4. E. M. Sparrow and J. L. Gregg, Laminar free convection from a vertical plate with uniform surface heat flux, *Trans. Am. Soc. Mech. Engrs* **78**, 435–440 (1956).
5. J. P. Dotson, Heat transfer for a vertical plate by free convection, MS Thesis, Purdue Univ. (1954).
6. R. Bill and B. Gebhart, The development of turbulent transport in a vertical natural convection boundary layer, to be published.
7. E. R. G. Eckert and T. W. Jackson, Analysis of turbulent free-convection boundary layer on flat plate, NACA TN1015 (1951).
8. E. Griffiths and A. H. Davies, The transmission of heat by radiation and convection, Brit. Food Investigation Board, DSIR, London, Spec. Rep. No. 9 (1922).
9. O. A. Saunders, Natural convection in liquids, *Proc. R. Soc. A* **172**, 55–71 (1939).
10. C Y. Warner and V. S. Arpaci, An experimental investigation of turbulent natural convection in air along a vertical heated flat plate, *Int. J. Heat Mass Transfer* **11**, 397–406 (1968).
11. F. J. Bayley, An analysis of turbulent free-convection heat transfer, *Proc. Inst. Mech. Engrs* **169**(20), 361 (1955).
12. R Cheesewright, Turbulent natural convection from a vertical plane surface, *J. Heat Transfer* **90**(1), 1–8 (1968).
13. C. S. H. Lock and F. J. de B. Trotter, Observations on the structure of a turbulent free-convection boundary layer, *Int. J. Heat Mass Transfer* **11**, 1225–1235 (1968).
14. B. Gebhart, Instability, transition, and turbulence in buoyancy induced flows, *Ann. Rev. Fluid Mech.* **5**, 213–246 (1973).
15. F. Godaux and B. Gebhart, An experimental study of the transition of natural convection flow adjacent to a vertical surface, *Int. J. Heat Mass Transfer* **17**, 93–107 (1974).
16. Y. Jaluria and B. Gebhart, On transition mechanisms in vertical natural convection flow, *J. Fluid Mech.* **66**(2), 309–337 (1974).
17 B. Gebhart and R. L. Mahajan, Characteristic disturbance frequency in vertical natural convection flow, *Int. J. Heat Mass Transfer* **18**, 1143–1148 (1975).
18. T. Audunson and B. Gebhart, Secondary mean motions arising in a buoyancy induced flow. *Int. J. Heat Mass Transfer* **19**, 737–750 (1976).
19. C. A. Hieber and B. Gebhart, Stability of vertical natural convection boundary layers: some numerical solutions, *J. Fluid Mech.* **48**, 625–646 (1971).
20. R. Dring and B. Gebhart, A theoretical investigation of disturbance amplification in external laminar natural convection, *J. Fluid Mech.* **34**, 551–564 (1968).

TRANSITION ET TRANSPORT POUR UN ECOULEMENT DE CONVECTION NATURELLE DANS L'EAU ADJACENTE A UNE SURFACE VERTICALE AVEC FLUX UNIFORME

Résumé—Cette expérience avec de l'eau à température ambiante montre avec précision le changement de la distribution de température moyenne depuis l'écoulement laminaire jusqu'à l'écoulement turbulent en passant par la transition. On détermine aussi les niveaux de perturbation de température. Simultanément des mesures très précises des paramètres du transfert thermique local sont faites à des nombres élevés de Rayleigh. L'objectif était de reconsidérer des critères connus pour le commencement de la transition thermique et de trouver une configuration caractéristique pendant la transition. On trouve que les critères sont cohérents un par un mais que quelques uns sont en désaccord avec d'autres à cause des différences dans la méthodologie. Des résultats pendant la transition peuvent être formulés en termes de profils moyens et de transfert thermique. Le transport en écoulement laminaire, de transition et turbulent est représenté. Dans le premier régime, il y a accord avec la théorie et dans le dernier avec la formulation de Vliet et Liu [1]. Les distributions moyennes dans la turbulence développée sont en accord étroit avec la nouvelle théorie de George et Capp [2].

ÜBERGANGSGEBIET UND TRANSPORT EINER AUFTRIEBSSTRÖMUNG IN WASSER NAHE EINER SENKRECHTEN OBERFLÄCHE MIT GLEICHMÄSSIGER WÄRMESTROMDICHTE

Zusammenfassung—Dieses Experiment mit Wasser bei Raumtemperatur gibt Änderungen in der Verteilung der Mitteltemperatur im Bereich von laminarer Strömung und im Übergangsgebiet bis zur vollständig turbulenten Strömung genau wieder. Das Ausmaß der Temperaturstörungen wurde ebenfalls bestimmt. Gleichzeitig wurden sehr genaue Messungen der Wärmeübergangsparameter bis zu hohen Rayleigh-Zahlen durchgeführt. Unser Ziel war es, verschiedene Kriterien für den Beginn des thermischen Übergangs untereinander in Beziehung zu bringen und alle charakteristischen Muster des Übergangs zu finden. Es wurde gefunden, daß diese Kriterien in sich konsistent sind, jedoch weichen einige wegen methodischer Unterschiede systematisch von anderen ab. Mittlere Profile und Transport sind relativ unzweideutig. Außerdem können auch einige Erscheinungen des Übergangs in Wechselbeziehung gebracht werden, sowohl hinsichtlich der mittleren Temperaturprofile als auch des Wärmeübergangs. Der Transport in laminarer Strömung im Übergangsgebiet und in turbulenter Strömung wurde dargestellt. Im ersten Bereich stimmt er mit der Theorie und im letzten mit der Korrelation von Vliet und Liu [1] überein. Verteilungen der Mitteltemperatur bei vollständiger Turbulenz sind in guter Übereinstimmung mit der neuen Theorie des Transportes von George und Capp [2].

ПЕРЕХОДНЫЕ ПРОЦЕССЫ И ПЕРЕНОС ТЕПЛА В СЛОЕ ВОДЫ, ПЕРЕМЕЩАЮЩЕЙСЯ ПОД ДЕЙСТВИЕМ ПОДЪЁМНЫХ СИЛ У ВЕРТИКАЛЬНОЙ РАВНОМЕРНО НАГРЕВАЕМОЙ ПОВЕРХНОСТИ

Аннотация — Описываемый эксперимент с водой при комнатной температуре позволил получить точную картину изменения среднего распределения температур при переходе от ламинарного течения к полностью развитому турбулентному течению, а также определить пороги температурных возмущений. Одновременно проводились точные измерения параметров локального теплообмена вплоть до больших значений числа Релея. Данное исследование ставило своей целью установление взаимосвязи между различными ранее предложенными критериями возникновения теплового нестационарного режима и выявление присущих переходу характерных картин течения. Найдено, что в основном большинство критериев совпадает, за исключением нескольких, что объясняется различием в методике проведения экспериментов. Соответственно наблюдается расхождение в средних профилях и значениях величин переноса. Кроме того, некоторые из наблюдаемых при переходе эффектов можно описать на основе результатов наших измерений с помощью средних профилей и значений по теплообмену. Получены профили переноса при ламинарном, переходном и турбулентном течениях. В первом случае данные по переносу согласуются с теоретическими результатами, а в последнем с обобщенным соотношением Влайета и Лиу [1]. Средние распределения температур при полностью развитом турбулентном режиме очень близко совпадают с результатами новой теории переноса, предложенной Джорджем и Кэппом [2].